

A Numerical Study of Coaxial Helical Antennas

William Coburn

U.S. Army Research Laboratory
Adelphi, MD 20783
wcoburn@arl.army.mil

Abstract– A FEKO model was constructed to investigate two helical antennas integrated coaxially on a shaped ground plane. One antenna was designed to have a reasonable gain and axial ratio (AR) from 0.5 – 0.9 GHz and the other from 1.0 – 1.6 GHz. In principle, the antennas could be connected in parallel to provide a near 50 Ω input impedance and act as a wideband antenna. However, this connection is problematic and can make fabrication more complex while changing the input impedance in unpredictable ways. An alternative is to use a microstrip impedance transformer to provide a 50 Ω input to each antenna. Then a broadband splitter can be used for a single feed wideband antenna. Otherwise, these two ports with switched input allow dual-band operation. The FEKO model is described and simulation results are presented for both cases. These results encourage further virtual prototyping and prototype fabrication for model validation.

Index Terms– Helical antenna, circular polarization, dual-band, fiberglass, Method of Moments, FEKO

I. INTRODUCTION

An axial mode helical antenna is often a good candidate when circular polarization (CP) is required over a moderate bandwidth (BW). The classical design is well established with design equations and measured data readily available [1]. The FEKO (www.FEKO.info) model, design procedure and fabricated prototypes are described in a companion paper for the low frequency helix (LFH) [2]. That paper describes a helical conductor embedded in thin fiberglass and mounted to a shaped ground plane with the antenna having a hollow core. It may be possible to take advantage of this empty space by

incorporating a high frequency helical (HFH) antenna, shown in Fig. 1.

To this end a FEKO model was constructed to investigate two helical antennas integrated coaxially on a shaped ground plane. The LFH was designed to have reasonable gain and axial ratio (AR) over a 0.5 – 0.9 GHz BW while the high frequency helix (HFH) was designed for a 1 – 1.6 GHz BW. In these frequency bands the propagation mode on each antenna is the fundamental axial mode with coupled modes similar to the bifilar helix [3]. The antennas could be connected in parallel to provide near 50 Ω input impedance and act as a potential wideband antenna allowing for perturbed radiation patterns. However, this connection can make fabrication more complex and changes the input impedance unpredictably. An alternative is to use a microstrip impedance transformer to provide a 50 Ω input to each antenna. Then a broadband splitter can be used for a single feed wideband antenna. Otherwise, these two ports with switched input allow dual-band operation.

In this paper, the FEKO model is described and numerical results are presented for both cases subject to assumptions about the dielectric properties of materials used in the prototype fabrication. The thin dielectric sheet (TDS) or coated wire approximations are options in FEKO suitably representing the helix embedded in thin fiberglass. The fiberglass thickness is $\sim 1/16$ -inch whereas the embedded conductor is $1/4$ -inch in diameter so it is a difficult antenna structure to model exactly. The results presented are for the coated wire approximation which is more computationally efficient than the TDS while providing similar results. An ideal embodiment, without dielectrics, is considered in addition to the laminated fiberglass fabrication. The results encourage further virtual prototyping to improve performance and fabrication for model validation.

II. FEKO MODEL

The FEKO model and classical design procedure for a 500 – 900 MHz axial mode helix were described in a companion paper and summarized here. This low-frequency helix (LFH) was designed for a center frequency of operation, $f_a = 700$ MHz corresponding to a free space wavelength, $\lambda_a = 16.87$ -inch. The resulting antenna is a 5-turn helix with pitch angle, $\alpha_a = 15.4^\circ$ having diameter $D_a = 5.56$ -inch and an axial length of 2 feet. The shaped ground plan has diameter, $D_g = 0.76\lambda_a = 12.75$ -inch with an edge height $\lambda_a/4 = 4.22$ -inch to which a thin fiberglass outer shell is attached to protect the antenna. The helical element is hollow copper tubing with diameter $\frac{1}{4}$ -inch laminated with 4-layers of fiberglass mat and cured using polyester resin. The FEKO model approximates this construction by a helical conductor wound for right-hand circular polarization (RHCP) with the coated wire approximation in FEKO used as a computationally efficient way to represent the thick conductor embedded in thin fiberglass.

The classical helix design has primarily resistive input impedance near 140Ω and is typically matched to 100Ω [4]. The FEKO model includes a linear tapered microstrip impedance transition (3-inch in length) from 50 to 100Ω so in all cases the simulations correspond to $50\text{-}\Omega$ source impedance. The helical conductor embedded in fiberglass shifts the gain BW to lower frequencies proportional to the fiberglass dielectric properties and thickness. This shift is predicted and can be approximately modeled in the Method of Moments (MoM) by a fiberglass coating on a helical conductor subject to the thin-wire approximation. The antennas considered here are modeled without dielectrics or using the electrically thin coating approximation in FEKO. The cured fiberglass laminate contains about 20% resin and is modeled with relative permittivity, $\epsilon_r = 4.5$ and loss tangent, $\tan\delta = 0.02$. These parameters are estimates based on measurements which indicate that typical cured resin systems have large loss at microwave frequencies on the order $\tan\delta \sim 0.1$ [5]. The resin dominates the dielectric losses so with 20% resin content the effective loss is taken as $\tan\delta = 0.02$.

A higher frequency helix on a shaped ground plane, designed for operation from 1 – 1.6 GHz is shown in Fig. 1. It is supported by a 3-inch thick nylon base. This structure is modeled in FEKO using the Finite Element Method (FEM) with $\epsilon_r = 3.2$ and loss tangent, $\tan\delta = 0.01$. This HFH has diameter $D_b = 2.7$ -inch, so it can fit inside the lower frequency helix (Fig. 1(b)) which is also supported by a 3-inch thick nylon base. The 2-ft axial length is maintained for the HFH with 10 turns leading to $\alpha_b = 15.8^\circ$. The shaped ground plane design was based on the LFH so the edge height is roughly twice the quarter-wave height that would be more optimal for the HFH. The calculated S_{11} for HFH only with and without dielectrics is shown in Fig. 2. The addition of fiberglass lowers the antenna resistance by $\sim 20 \Omega$ without a significant change in the input reactance, so the return loss is reduced ~ 1 dB.

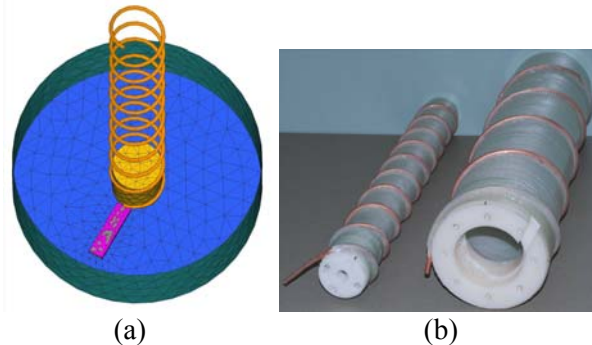


Fig. 1. (a) FEKO HFH model with nylon base on shaped ground plane and (b) the HFH (left) and LFH (right) fabricated prototypes.

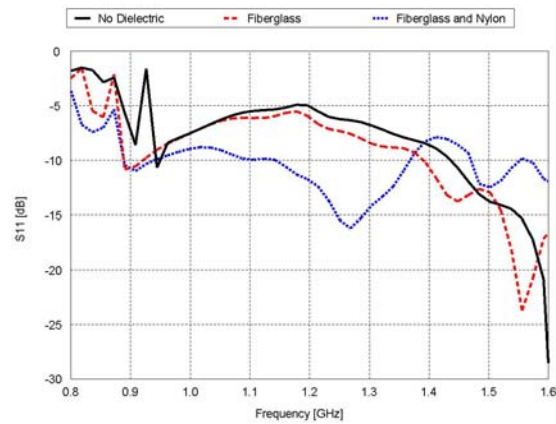


Fig. 2. Calculated S_{11} for the HFH only with and without dielectric loading.

The input impedance variation due to the effect of the nylon base, attached to the ground plane, is more pronounced and cannot be neglected. The impedance transformer substrate (RT Rogers/Duroid 5880) and the nylon base are modeled using the FEM while the fiberglass is included using the coated wire approximation. The RHCP realized gain (in dBic) shown in Fig. 3 is on the helix axis, or boresight, where the reduced gain around 1.2 GHz was roughly independent of the dielectric loading. Selected patterns for the HFH only with all dielectrics included are shown in Fig. 4.

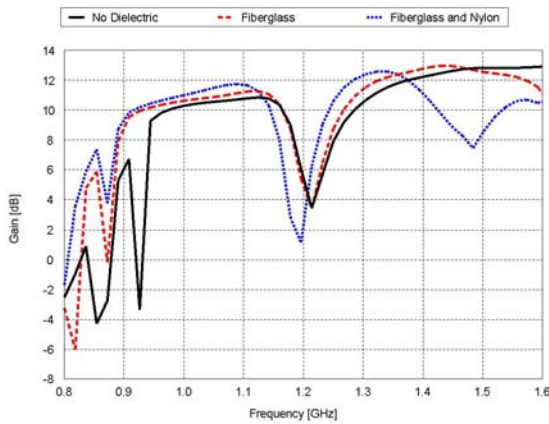


Fig. 3. Calculated RHCP realized gain on boresight for the HFH only with and without dielectric loading.

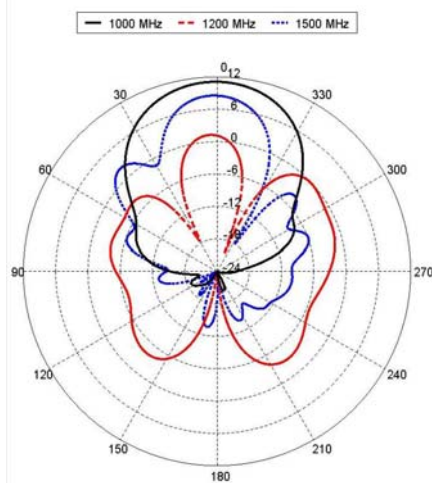


Fig. 4. Calculated RHCP realized gain patterns for the HFH only with dielectric loading.

The reduced gain at 1.2 GHz is associated with the ground plane edge height. This null can be improved and shifted in frequency by reducing

this edge height as shown in Fig. 5. The original model compared to one having half the ground plane height has the same 90% efficiency but has drastically different radiation patterns. This change could introduce pattern perturbations at low frequency and is a parameter to optimize in the future for the dual helix configuration.

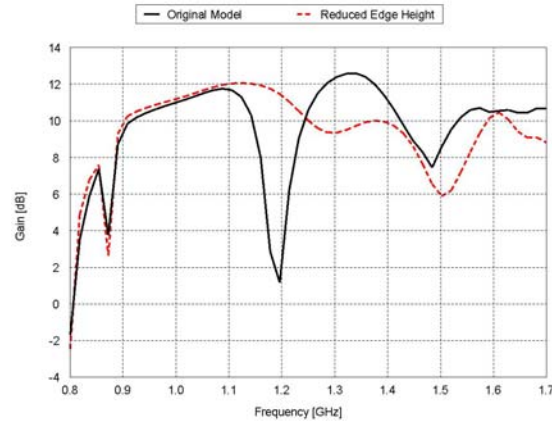


Fig. 5. RHCP realized gain comparison for the HFH only with reduced ground plane edge height.

The LFH and HFH models are combined in a coaxial arrangement as shown in Fig. 6. A gap in the LFH nylon base is provided to attach the microstrip transformer output to the HFH input. The input connectors are attached to the bottom of the ground plane directly below the transformer inputs with pins connected directly to the microstrip. These connections are modeled using a thin wire which in FEKO cannot lie on a dielectric surface and must connect to a part of the microstrip that extends beyond the Duroid substrate. The helix is also connected with a thin wire since the height of the first turn above the ground plane is slightly larger than the 1/4-inch substrate thickness (Fig. 6(b)).

These ports are driven simultaneously or individually to demonstrate different excitation options. Selected FEKO model results for both modes are shown where a passive splitter feed is modeled by exciting both antennas simultaneously with equal amplitude and phase. Wires wound for RHCP are used to model both the helical conductors in the same manner. For the desired segmentation the 1/4-inch conductor does not satisfy the thin wire approximation so a wire radius, $a = 0.1$ -inch rather than the actual, $a = 0.125$ -inch was used in simulations. In addition,

the uncertainty in the dielectric properties also contributes to the physical modeling error.



Fig. 6. Dual helix antenna (a) FEKO model with nylon supports and (b) impedance transformer input model.

III. WIDE-BAND OPERATION

When connected in parallel, the dual helix antenna has input resistance near 70Ω and could be driven with 50Ω source impedance. Such a connection complicates the fabrication and introduces parasitic reactance. To circumvent this problem, the simulation includes an impedance transformer on both inputs which are driven simultaneously. This two-port model then represents feeding both inputs with a splitter and matched cable lengths to be in-phase with equal amplitude. The results for the LFH helix (port 1) and the HFH helix (port 2) are shown in Figs. 7 and 8 respectively. The wideband helix with dielectric loading is reasonably well matched to 50Ω , but the patterns become corrupt at higher frequency having reduced gain on boresight owing to a tilted or split main beam.

The realized gain on boresight (in dBic) versus frequency is shown in Fig. 9. Without dielectric loading, the results indicate only a small dip in the boresight gain near 1.2 GHz. This dip is similar to the HFH only simulation (see Fig. 3). With dielectric loading this boresight null increases and is shifted to near 1.4 GHz. At this frequency the wideband antenna has 79% efficiency with $\sim 12\%$ dielectric losses compared to the no dielectric case with 87% efficiency from mismatch loss. With increasing frequency the boresight gain drops due to a combination of dielectric losses and the onset of the HFH conical mode radiation. The null on boresight near 1.4 GHz is not nearly the pattern perturbation associated with the ground plane edge as in the HFH alone (Fig. 4). This frequency dependence appears to be a combination of mutual

coupling and dielectric loading effects which reduces the antenna efficiency and at some frequencies leads to a split main beam.

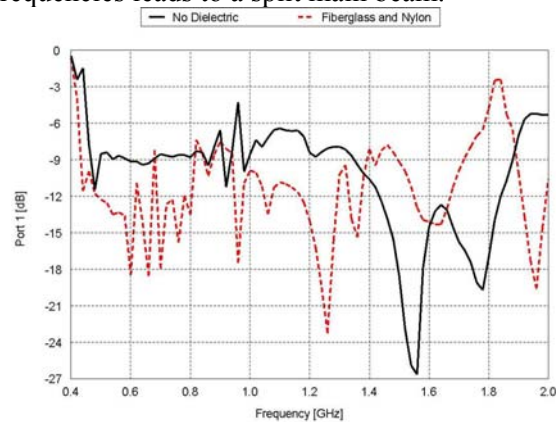


Fig. 7. Calculated S_{11} for the wideband helix antenna with and without dielectric loading.

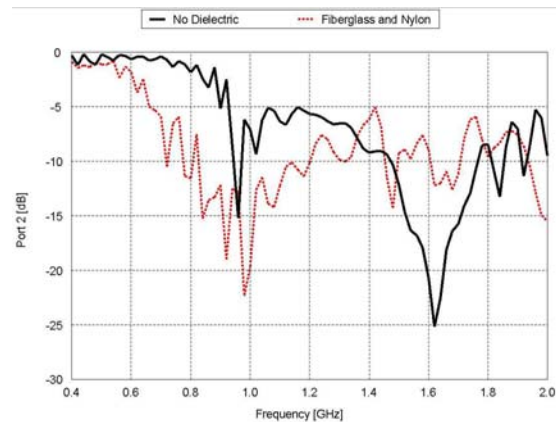


Fig. 8. Calculated S_{22} for the wideband helix antenna with and without dielectric loading.

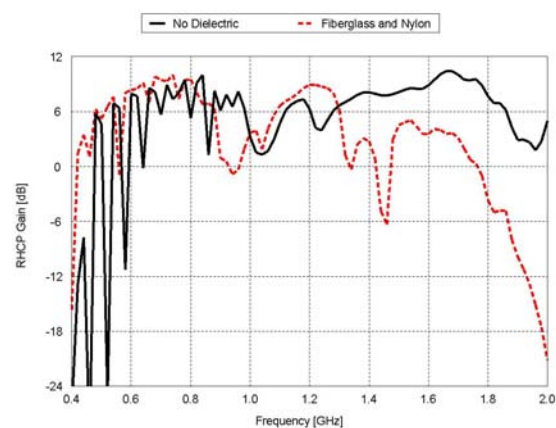


Fig. 9. Calculated RHCP realized gain for the wideband helix antenna on boresight.

The RHCP patterns at selected frequencies are shown in Fig. 10 with dielectrics included showing the off-boresight radiation at some frequencies. The patterns have more side lobes and back lobes than a single helical antenna. For wideband operation a microstrip corporate feed system could be designed to fit in the available space remaining on the ground plane. The opposed arrangement of the feed points, which for the HFH must then protrude through the outer nylon base (see Fig. 6), makes such a design complicated and was not pursued.

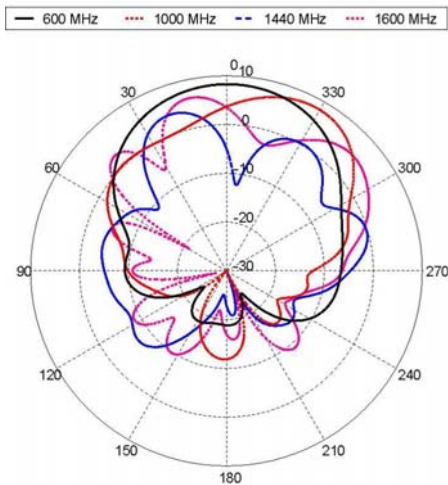


Fig. 10. Calculated RHCP realized gain patterns for the wideband helix antenna.

IV. DUAL-BAND OPERATION

The coaxial helical antenna could also be operated as a dual-band antenna using a microstrip transformer on each helix to provide two 50 Ω input ports. In this configuration, each port is driven separately, with the other port terminated into 50 Ω and the plotted simulation results overlap from 900 – 1100 MHz. The calculated S-parameters are shown in Fig. 11 with the fiberglass coating and nylon support structures. As with the high frequency helix by itself, including dielectrics with the dual helix improves the return loss somewhat. Thus, the antennas could be switched at 900 MHz and maintain reasonable return loss over the entire 500 – 1600 MHz BW. The isolation (S_{12}) between these antennas is not very good over most of the frequency band with the strongest coupling in the low frequency region where only the LFH is excited. Only an opposed

feed arrangement was investigated, so this geometry may not be optimum and is an area for future study.

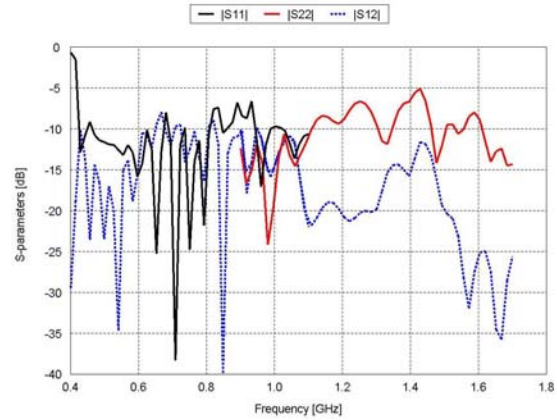


Fig. 11. Calculated S-parameters for the dual-band helix antenna with dielectric loading.

The realized gain versus frequency on boresight is shown in Fig. 12 (with and without the nylon support structures) showing the overlapping performance around 1 GHz. The gain BW has a gap with reduced gain from 900 – 1100 MHz even though the impedance BW indicates better performance. This is because both the LFH and HFH peak gain is reduced and can be off-boresight in the frequency range near the band edges. Similarly, the HFH peak gain is off-boresight at some frequencies with a split main beam near 1450 MHz. Example patterns for the original model with the fiberglass coating and nylon structures included are shown in Fig. 13.

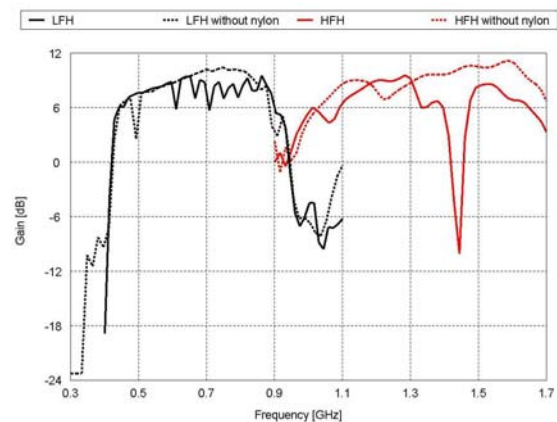


Fig. 12. Calculated RHCP realized gain for the dual-band antenna with and without nylon base.

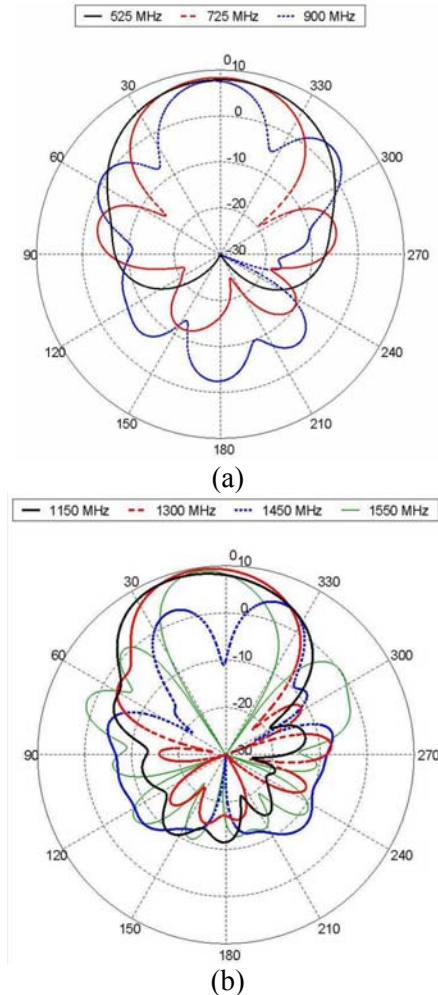


Fig. 13. Calculated RHCP radiation patterns for the dual-band helix antenna with dielectric loading for the (a) LFH driven and the (b) HFH driven.

Several methods of feeding the HFH were evaluated empirically and most techniques were found to introduce unwanted inductance. The best method installed the connector underneath and as close as possible to the transformer in order to avoid any wire connections. With this approach, the antenna input impedance is marginal but the results encourage further optimization. The dielectric support structures, the location of the feed regions and the ground plane edge height are all design features that this study found to impact performance. Future efforts can attempt to optimize such features both individually and in combination to improve the results shown here.

Nylon in the feed region has a large detrimental effect on the HFH performance. To

further investigate this influence, the LFH transformer was removed so this port is open-circuited. This baseline model runs faster while still having the dominant features of the boresight gain versus frequency as in Fig. 12. However, the split beam at some frequencies is not observed for the LFH open-circuit implying that this pattern perturbation is a mutual coupling effect when the non-driven port is terminated. We investigated variations of the simplified model in an attempt to identify design parameters that have the largest impact on performance. Two such variations are summarized here. First, the height of the nylon supports is reduced by a factor of two (1.5-inch). Then the ground plane edge height is also reduced by a factor of two (2.11-inch). The comparison is shown in Fig. 14 for the boresight gain versus frequency indicating that the dielectric loading in the HFH feed region is the primary cause of the reduced gain on boresight near 1460 MHz. The input impedance mismatch dominates the antenna efficiency where the loss in the nylon is larger than that in the coated wires. The baseline model is only 4% less efficient, but the dielectric loading tilts the beam off boresight at some frequencies.

Radiation patterns for the baseline model compared to these two variations are shown in Fig. 15 at 1460 MHz. Notice that the baseline model with the LFH open-circuit has a tilted rather than split beam with >6 dBic main beam gain reduction. This numerical study indicates that a smaller or different dielectric support structure should be considered after which the ground plane design can be optimized for dual-band operation.

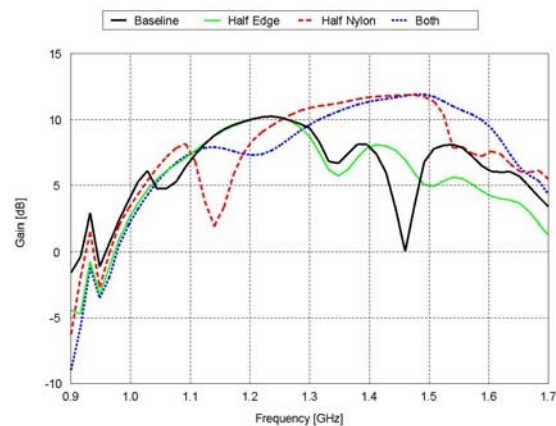


Fig. 14. Calculated RHCP realized gain on boresight with the LFH open-circuit.

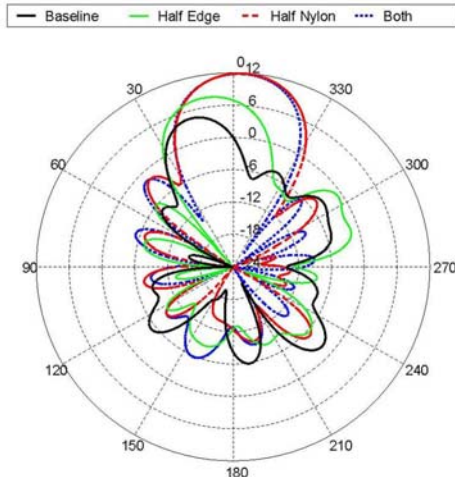


Fig. 15. Calculated RHCP patterns with the LFH open-circuit at 1460 MHz.

As an example of design improvements, the ground plane edge and nylon base heights are both reduced by a factor of two in the dual-band helix model. This simulation confirms that design changes which improved the HFH boresight gain are not detrimental to the LFH performance. The return loss and boresight gain comparisons for the original and revised design are shown in Figs. 16 and 17 respectively. The results indicate that dielectric loading is an important parameter for the antenna input impedance. Less nylon improves the LFH and HFH efficiency over most of their in-band frequencies. At 1428 MHz the efficiency increases by 30% when reducing the nylon and edge height owing in part to 11% less loss in the nylon. Less nylon in the HFH feed region and reduced edge height also improves the input impedance mismatch by 19% with less pattern perturbations compared to the original model.

Pattern comparisons at selected frequencies are shown in Fig. 18. Obviously, these changes improved the design and will be the basis for further optimization. Additional tradeoff studies in the materials selected for the helix supporting structures can be conducted numerically. Further optimization of the feed region details and ground plane design could lead to additional performance improvements.

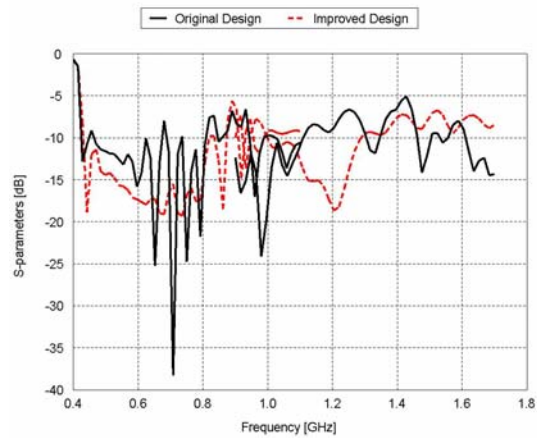


Fig. 16. Calculated S-parameters for the original and revised dual-helix antenna designs.

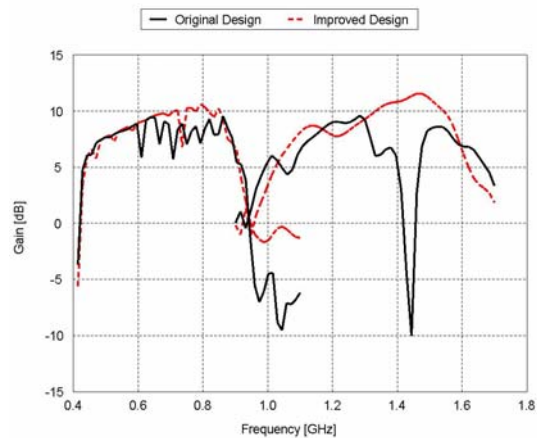


Fig. 17. Calculated RHCP realized gain on boresight for the original and revised design.

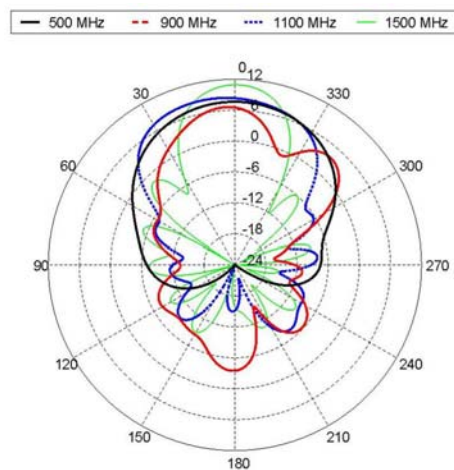


Fig. 18. Calculated RHCP radiation patterns for the improved dual-band helix design.

V. CONCLUSIONS

The results shown for the wideband and dual-band approaches encourage further virtual prototyping and prototype fabrication for model validation. Both approaches have reasonable performance; however, at frequencies near the band edges the peak gain can be $15^\circ - 30^\circ$ degrees off-boresight. A null in the boresight gain near 1200 MHz is observed with the HFH only which depends on the ground plane edge height as can be seen in Fig. 5. The ground plane design was based on an optimum quarter-wave edge height [1] for the LFH but reduced the boresight gain at some frequencies for the HFH alone.

The numerical study progressed from simple models of the HFH only to the LFH/HFH coaxial antenna while including more feed region details and dielectric structures subject to the FEKO approximations and limitations. It was found that even for thin fiberglass the dielectric loading was an important effect tending to shift the antenna impedance and gain BW to lower frequencies with reduced gain at high frequency. The influence of the nylon base supports significantly impacted the antenna performance introducing more frequency dependence, reduced boresight gain, and perturbed radiation patterns. The model could be refined even further by using measured dielectric properties as a function of frequency. However, the helical conductors embedded in thin fiberglass cannot be modeled exactly. Rather, the coated wire approximation is used because it is efficient and approximates measured results.

The dual-band model has two feed regions with transformers in opposed positions with the Duroid and nylon modeled using the FEM. This represents more accuracy but requires more computational resources and takes ~10 minutes per frequency or roughly 6 hours per simulation. The dual-band simulation requires two runs with overlapping frequencies to excite each port separately. Results over the full BW require ~12.5 hours. When driven simultaneously, the simulation time is reduced but the results have limited utility since such an idealized input model is difficult to achieve in practice.

The coaxial helix model was successfully used to investigate design improvements. It showed that by reducing the size of the nylon base plate and the ground plane edge height the antenna

performance can be improved. The model results indicate that fabrication alternatives can dramatically affect performance at high frequency. Even an approximate model is beneficial to evaluate relative differences in material selection and fabrication options compared to constructing and measuring multiple prototype antennas. Once validated to provide more confidence in the results, the FEKO model can be used to further optimize the dual-band antenna performance.

REFERENCES

- [1] H. E. King, J. L. Wong, and E.H. Newman, "Helical Antennas," *Antenna Engineering Handbook*, 4th Ed., J. L. Volakis (ed.), Chap. 12 (New York: McGraw-Hill, 2007).
- [2] W. Coburn, C. Ly, T. Burcham, R. Harris and A. Bamba, "Design and Fabrication of an Axial Mode Helical Antenna," Proceedings of the 2009 ACES Conference (March 2009).
- [3] J. R. Pierce and P. K. Tien, Coupling of Modes in Helices, Proceedings of the IRE, Vol. 42, pp. 1389–1396 (September 1954).
- [4] J. D. Kraus, "The Helical Antenna," *Antennas*, Chap. 7 (New York: McGraw-Hill, 1950).
- [5] R. B. Bossoli, "The Microwave Permittivity of Two Sprayable Resin Systems," U.S. Army Research Laboratory, ARL-TR-3907, September 2006.



William O'Keefe Coburn received his BS in Physics from Virginia Polytechnic Institute in 1984. He received an MSEE in Electro physics in 1991 and Doctor of Science in Electromagnetic Engineering from George Washington University (GWU) in 2005. He has 28 years experience as an electronics engineer at the Army Research Laboratory (formerly the Harry Diamond Laboratories) primarily in the area of CEM for EMP coupling/hardening, HPM and target signatures. He currently is in the RF Electronics Division of the Sensors and Electron Devices Directorate applying CEM tools for antenna design and analysis.